

Deep Boreholes for Storage of Spent Reactor Fuel and Use of the Heated Rock for Production of Electric Energy or hot fluid for heating purposes

Roland Pusch¹, Richard Weston² and Jörn Kasbohm³

Abstract

Lack of energy is a serious threat to the prosperity of many developed states that have access to or plan to use nuclear power. The paper describes a concept for solving two major problems related to these conditions, namely safe disposal of spent reactor fuel and generation of electric energy or hot fluid by use of heat produced by the disposed waste. The challenge in storing spent nuclear fuel can be met with by installing such highly radioactive waste in deep boreholes with fuel rods encapsulated in canisters of copper-lined iron or titanium. Electric energy can be generated by utilizing the accumulated heat in the same rock mass by pumping up hot water or clayey mud from series of deep holes bored parallel and between corresponding holes with nuclear waste. The amounts of heat in each of the hot-water holes overlap and raise the initial rock temperature at 1,500-3,000 m depth to about 80-90°C after some 50 years and to 70-80°C in 500 years, after which the temperature in the hot-fluid holes goes down successively to the initial value 60-70°C in about 500 years. If these holes are subsequently deepened from 3,000 to 5,000 meters, utilization of the hot fluid can continue for another 500 years.

Keywords: Deep boreholes, highly radioactive waste, high level radioactive waste (HLW), spent reactor fuel, smectite, clays.

¹ Luleå University of Technology, Geotechnical Division, Sweden.

² Dep. of Production and Materials Engineering, Lund University, Sweden.

³ Geographical and Geological Dept, Greifswald University, Germany.

1. Introduction

The nuclear energy cycle comprises refinement of uranium dioxide for manufacturing nuclear reactor fuel of type U-238, generation of heat in the fission process in nuclear reactors, and disposal of the rest product. Experience demonstrates that the energy output can be predicted for each weight unit of the fuel. The heat generated will be dispersed through the waste canisters and their embedment into the surrounding rock. The repositories can consist of very deep (3-5 km) or long flat-lying boreholes (A and D in Figure 1) or be mined (B and C) with short holes bored from tunnel floors for placement of canisters at a few hundred meters depth. In this document we focus on storage of spent reactor fuel in deep holes (Case A).⁴

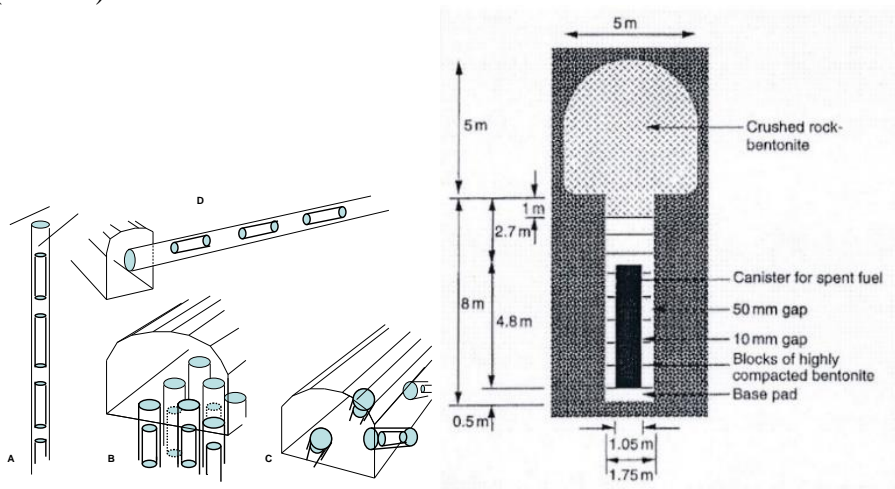


Figure 1: Repository concepts for permanent disposal of highly radioactive waste (Left), and SKB's¹ concept for disposal of spent reactor fuel at about 400m depth (Right). (Pusch, 2008).

⁴ Swedish Nuclear Fuel and Waste Management Co

2. Scope of Study

The main idea of the study is to find out the conditions for combining the concept of deep disposal of highly radioactive waste in the form of spent reactor fuel for heating crystalline rock sufficiently much to utilize the accumulated heat for production of electric energy by pumping up hot groundwater from series of deep holes bored parallel and between corresponding holes containing nuclear waste.

The working principle is schematically shown in Figure 2 and similar to that of the Enhanced Geothermal System (EGS) proposed by the US company GreenFire Energy Co. The difference is that the presently presented concept uses disposed nuclear waste in the form of spent reactor fuel for heating rock in which bored deep holes pick up the heat energy and uses it for generating electricity or heating buildings via heat exchangers, while EGS makes use of the natural heat in very deep boreholes. The double function of the present concept reduces the net cost of disposal of highly radioactive waste and provides electric energy or hot water or vapour for heating purposes. The holes can be up to 5km deep, but we confine ourselves here to deal with 3km deep holes.

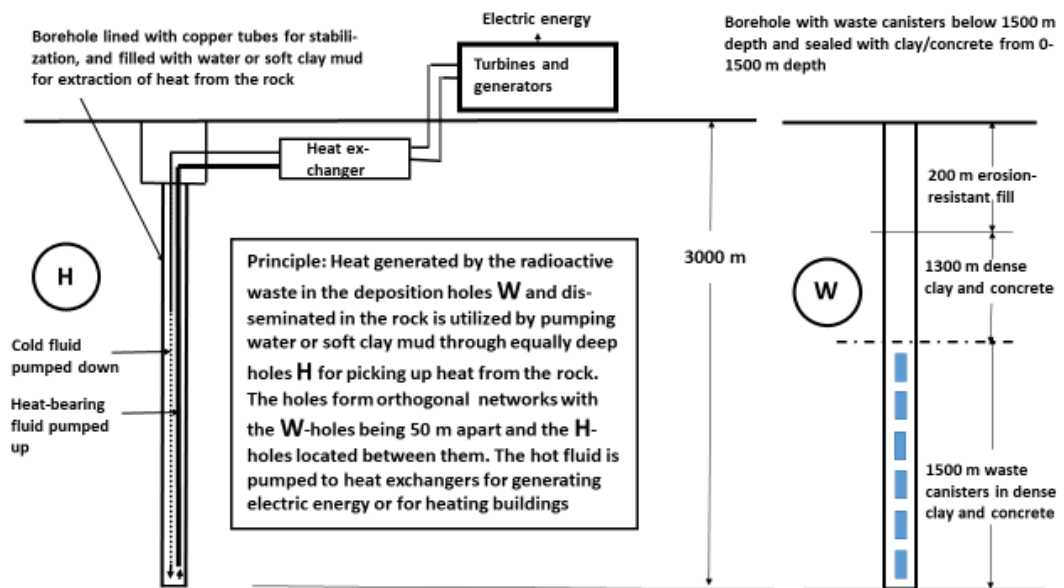


Figure 2: Schematic description of the function of the presently proposed concept for final disposal of highly radioactive waste in the form of spent reactor fuel and utilization of heat generated by such waste for energy production.

3. Function of the geothermal system

3.1 The disposed spent nuclear fuel

The proposed geothermal system of regularly spaced 3,000m deep boreholes with 0.5 to 0.6m diameter with heat-generating high-level radioactive waste (HLW) in the form of spent nuclear fuel contained in canisters in the lowest 1,500m part (depth 1,500-3,000m), consists of two sets of very deep boreholes. The working principle is that the nuclear waste in one of the systems warms the surrounding rock and thereby the other system of boreholes with 0.2-0.3m diameter filled with water or soft smectitic clay mud in which closed pipe loops are inserted. The fluid in them will have a temperature of 70-80°C and is directly pumped into heat exchangers that alters the temperature to a level that is suitable for running turbines and generators for producing electricity or water/vapor for heating buildings. The system is depicted in Figure 2 in which a hole for disposal of spent nuclear fuel denoted W. Figure 3 shows a plan of the integrated systems of boreholes. The spacing of the holes for radioactive waste charged to give an energy of at least 600W is taken here as 50m while that of the hot-fluid holes is assumed to be 25m. These spacings imply acceptable overlap of the heat plumes from the waste-bearing holes and minimum risk of interference of the hot-water holes.

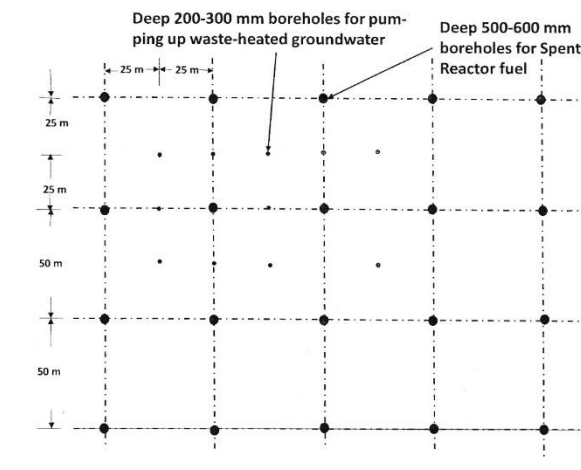


Figure 3: Borehole placement for combined waste disposal and use of heat from disposed nuclear reactor fuel. The wide holes for waste disposal have a spacing of 50m while the smaller ones with 25m spacing are used for pumping up groundwater heated by the nuclear waste.

3.2 Exploitation of the heat from the waste

The heat generated by the disposed fuel in a system of deep boreholes is picked-up by circulating groundwater in a second, integrated system of equally deep boreholes in the same rock volume for generating electric energy in powerhouses on the ground surface or at a limited depth in the rock. This concept is a combination of a series of deep vertical boreholes with 500mm diameter and 3km depth for disposal of spent fuel in their lower 1.5km part and an integrated system of boreholes with 400-500 mm diameter boreholes reaching down to 3 km for circulating groundwater to heat exchangers located on the ground surface or at shallow, safe depth as indicated in Figure 2 in which a hot-fluid hole is included ("H"). Heat from the nuclear waste will fade off significantly in a couple of centuries but the function of the hot water holes can be prolonged by deepening them by 1km for utilizing the natural heat of deeper rock.

A somewhat similar repository concept was worked out by the Swedish construction company Widmark and Platzer in cooperation with SKB several years ago (Svemar, 2005a). It consisted of a central vertical shaft and numerous boreholes connecting tunnels and boreholes extending from it for HLW. The system would be surrounded by a hydraulic cage with an outer diameter of 230m and a height of 450m, the distance to the central shaft filled with clay/sand "buffer" material being 50m. The hydraulic cage surrounding the repository part was claimed to be used for providing heat energy for production of electric energy, but the hydraulic and mechanical functions of the repository rock would be largely unpredictable by the very high temperature gradients in the rock intercepted by the high number of holes and tunnels. Another weak point of this concept was that the repository was assumed to be kept drained for 100 years, which would desiccate the fine-grained rock fill in the canister holes and promote fracturing of the repository host rock.

3.3 Location

The system of boreholes should be in the neighborhood of a community or medium-size town for providing heat from the nuclear waste for supplying the town with hot water for warming buildings, roads and pavements. Optimal location of the boreholes requires that the deep holes of the two borehole systems are located in rock with few major fracture zones since they have a potential to undergo shear strain which can largely change the mechanical stability of the rock mass and change the hydraulic performance. Figure 4 shows a schematic rock structural model of a site with different types of fracture zones termed 1st, 2nd, and 3rd order zones with the major properties listed in Table 1. Below 2,000m depth the average hydraulic conductivity is commonly lower than E-12m/s and the water pressure below 20MPa (Pusch et al, 2019).

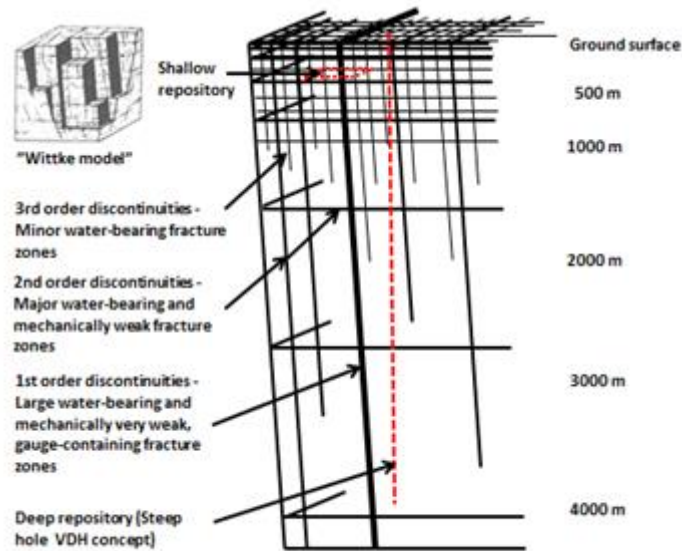


Figure 4: Simplified structural model of crystalline rock. The difference between mined (shallow) and very deep (VDH) repositories is obvious from the different frequencies of intersected 2nd and 3rd order water-bearing fracture zones for the respective concepts.

Table 1: Scheme for rock fracture zones with average hydraulic conductivities: VH=very high, H=high, M=medium, L=low, VL=very low, VVL=insignificant conductivity. Those of 4th to 7th orders are discrete fractures or narrow fracture zones with low average hydraulic conductivities (Pusch, 2019).

Order	Length	Hydraulic conductivity	Gouge content	Strength	D-system (SKB)
1 st	>Kilometers	VH	VH	VVL	D1
2 nd	Kilometers	H	H	VL	D2
3 rd	Hundreds of meters	M to H	M	M	D3
4 th	Tens of meters	M to H	L	H	D4
5 th	Meters	L	VL	H	-
6 th	Decimeters	VL	VL	VH	-
7 th	<Decimeters	VVL	VVL	VVH	-

4. Holes for disposal of HLW

4.1 Design and construction

Unlike mined repositories the prime engineered barrier separating HLW from the biosphere in VDH is the heaviness of deep groundwater, which can have the density of ocean water and calcium as major cation. The principle of VDH is to store HLW “supercontainers” in the lowest 1.5km deployment part of the holes (cf. Figure 5), while the uppermost part of them is plugged with moraine-graded quartzite stabilized by low-pH cement from the ground surface to 200 m depth, and effectively sealed from 200 to 1,500m depth by dense smectitic clay confined in supercontainers without nuclear waste. These are inserted piece-wise or in small series except where major water-bearing fracture zones are intersected or where significant rock fall has taken place requiring sealing by casting low-pH concrete. The concrete needs to be physically stable and low-permeable soon after casting (Muhammed et al, 2014). The tight seals preferably consist of smectite-rich clay in the form of highly compacted blocks, i.e. the same as being proposed by SKB for mined repositories (MR), cf. Svemar (2005a and b).

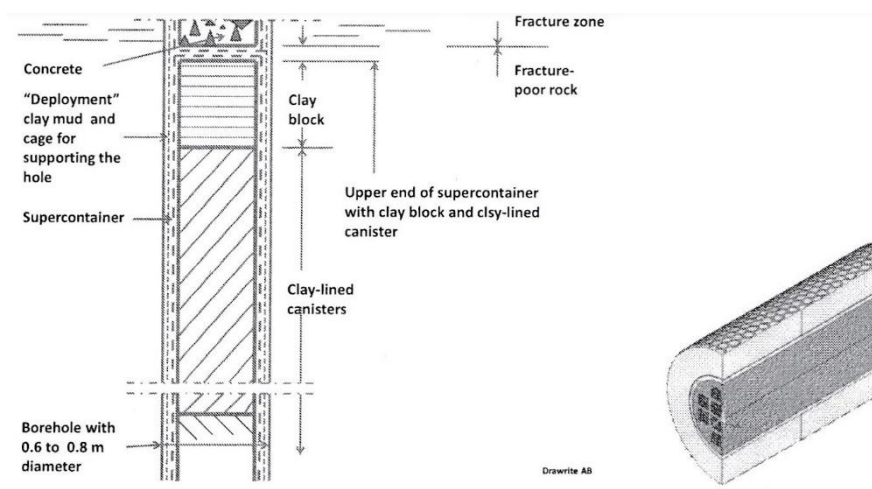


Figure 5: Design of VDH hole (Pusch et al, 2019). Left: Segments from 1,500 to 3,000 m depth. Right: Supercontainer with canister having channels for spent nuclear fuel and being tightly filled with very dense blocks of smectitic clay. The borehole diameter can be up to 0.8 m but is preferably 0.5-0.6 m.

Migration by heat-induced convection of possibly radioactively contaminated groundwater to less than 100m above the deployment zone (Pusch and Börgesson, 1992), would make sealing of only the uppermost part of VDH sufficient but the present concept implies the same type of supercontainers for sealing the entire segment between 200 and 1500m depth (cf. right part of Figure 5). Other hole diameters than 800mm considered by Brady and others (2009), are 840mm, 560mm, and 450mm for different charges of waste. The high temperature in the deployment

zone makes it necessary to consider the pressure and stability conditions as exemplified by 3km deep holes for which the static water pressure at their base will be about 30MPa while the effective pressure can be more than 45MPa when they are filled with medium dense clay mud, hence guaranteeing physically stable conditions for a maximum temperature of 150°C.

Taking Sweden as an example of a state with moderate use of nuclear power - it has 10 nuclear reactors with 1,000MW average power and 40-year intermediate storage of the spent fuel - successive disposal of canisters would be made in 20-25 years. Four to twelve multiple borehole sites were earlier considered to be required, each containing 4-5km deep holes with 200m spacing for avoiding thermal overlap. More recent thermal calculations show that the spacing can be reduced to 50m (Gibb, 2017). A few tens of years ago a suitable borehole diameter was estimated at about 800 mm, which may be at the limits of modern deep-boring capability. For holes with 3km depth a suitable diameter can be in the range of 500-600mm as they can accommodate a complete PWR assembly of spent fuel (Gibb, 2017). Here, we will still assume 800mm but confine ourselves to consider holes with a total depth of no more than 3km, containing spent fuel between 1.5 and 3km depth and clay seals with intermittent concrete plugs from a depth of 0.2km and downwards.

4.2 Function

Unlike mined repositories the prime engineered barrier separating HLW from the biosphere in VDH is the heaviness of deep groundwater. The principle of VDH is to store HLW in the 1.5km deep deployment part of the holes, and to effectively seal the upper parts of them with dense smectitic clay confined in the same type of supercontainers of copper or titanium as those in the deployment zone.

In Swedish bedrock the natural temperature rise with depth is in general 1.6-1.7°C per 100m depth, meaning that the temperature at the bottom of 3km deep holes may be slightly higher than 50°C before bringing waste canisters down, but significantly higher after installation of canisters with 4 BWR (boiling water reactor) elements, or 2 BWR and 1 PWR (pressure water reactor) elements, assuming common data for heat generation and thermal properties of the clay and granitic rock (Grundfeldt, 2010). The holes are assumed to be filled with smectite mud with a dry density of 150-250kg/m³ during boring and waste installation. An important matter is the concentration of total dissolved salt (TDS) content, which is about 100,000ppm in the groundwater at 3km depth, and that the density of the groundwater at this depth is so high that convective flow generated by the heat production will not bring possibly contaminated water higher up than 50-100m above the waste-containing part (Pusch and Börgesson, 1992). The Ca/Na ratio, which affects the microstructural state of clay seals is expected to be at least 2 deeper than 2km, while it is estimated to be 1.5 higher up.

Temperature calculations have been made applying different energy outputs from the encapsulated waste and using an appropriate commercial finite element code and the following thermal data for the rock: Density 2500kg/m³, Thermal

conductivity⁵ 1.5 W/(m K), Specific heat 774 J/(kg K). The results are shown in Figures 6-8, which indicate slight superposition of the respective heat pulses.

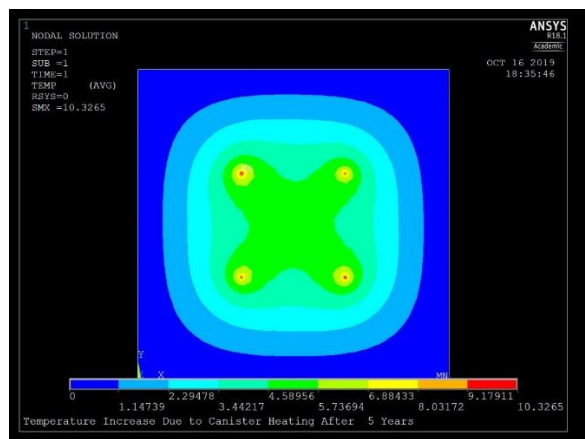


Figure 6: Temperature increase from the 600 W canister surfaces for a set of four canister holes 50m apart after 5 years. Maximum value is 10.33°C, which, for 70°C ambient temperature gives about 80.3°C total temperature . Beyond about 40m from the holes there is no temperature rise after 5 years. For the hot-water holes located between the big ones the rock temperature will be about 75°C.

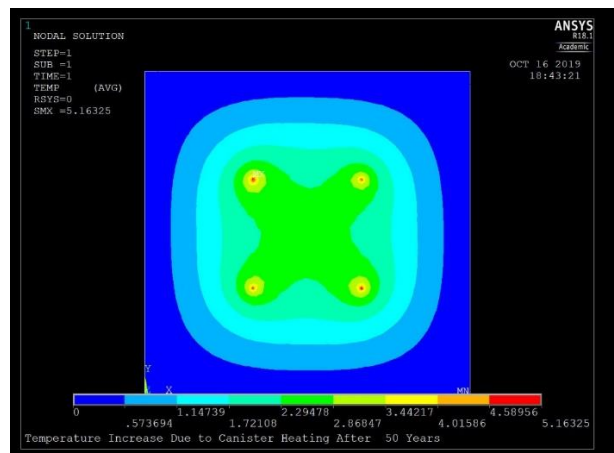


Figure 7: Temperature increase from the 600 W canister surface after 50 years. Maximum value is 5.16°C, which, for 70°C ambient temperature gives about 75.2°C total temperature after 50 years. For the hot water holes the rock temperature at this time will be about 72°C.

⁵ This figure is lower than the commonly cited data for granite (2-3W/mK) and gneiss (2W/mK) but on the same order as the thermal conductivity of amphibolite and the proposed clay mud. The assumed value is hence conservative with respect to the heat propagation ability of the system.

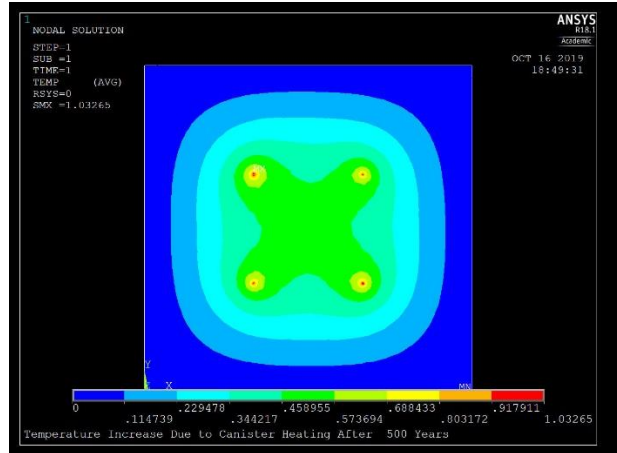


Figure 8: Temperature at the 600W canister surface for a set of four canister holes after 500 years. Maximum value is 0.92°C, which, for 70°C ambient temperature gives about 70.9°C total temperature implying some slight cooling after 50 years. For the hot water holes the rock temperature at this time will be about 70.5°C.

One realizes that the temperature of the hot-water holes stays fairly constant at 75-80°C in the first 50 years after sealing the holes with spent nuclear fuel and then slowly drops to 70°C after 500-1,000 years. The system of hot-water holes will hence represent a relatively constant heat source for generating electric power or warming buildings for a millennium.

4.3 Risk assessment

4.3.1 General

Some key processes and functions need to be judged for assessing the long-time function and safety conditions of a VDH disposal site. Here, we will consider the stability and function of the host rock and then focus on the clay components, paying also attention to the concrete seals.

4.3.2 Rock

As to the host rock, the thermal impact on the stability and hydraulic function of the nearfield of the holes with waste and generated hot water is deemed insignificant since the temperature span from waste installation to decay of heat generation is small and the stabilizing isostatic effect of the rock mass above and around the deployment zone is considerable. For the nearfield of the hot-fluid holes the stability of the rock will not be notably affected at all.

4.3.3 Buffer clay

4.3.3.1 General

The limited waste isolation capacity of the host rock requires use of engineered barriers in the form of metal canisters and dense clay seals. Clay is used for minimizing groundwater flow in the immediate surrounding of HLW canisters (“Buffer Clay”) and elsewhere in the repository, and also for providing the canisters with ductile embedment for minimizing the risk of damage by displacements in the host rock. It is manufactured by strong compaction of smectite granules yielding blocks with a shape that is suitable for placement where sealing is required. The dense blocks will swell in conjunction with water uptake until their full hydration potential has been utilized, which means that the blocks can expand even if they are water saturated from start (cf. Pusch, 2015, 2019).

The primary clay component is smectite-rich mud with which all the holes are filled before the supercontainers with dense clay and HLW are installed. Its most important functions are to provide mechanical support to the walls of the holes and to supply the dense clay in the supercontainers with water before the surrounding rock starts to furnish groundwater. The mud must be sufficiently low-viscous to let the heavy supercanisters slip down to the intended positions but enough quickly maturing to become low-permeable and physically stable for tens to hundreds of thousands of years. The matter is particularly important to the overall function of most HLW concepts and is treated here with respect to the function and longevity of three candidate clay types (Pusch and Yong, 2006; Kasbohm et al, 2012).

4.3.3.2 Criteria for the buffer clay

The geotechnical properties of clay barriers required for fulfilling the criteria is low hydraulic conductivity, sufficient mechanical strength and ductility and self-healing ability after undergoing expected compression, expansion and deformation in terms of creep strain under shear stresses. Table 2 exemplifies typical properties of three types of smectitic clay that will be referred to in this paper as candidate reference materials. The values stem from comprehensive tests of clay materials saturated with low-electrolyte water and 1-3.5% CaCl₂ solution. The swelling pressure is a practical measure of the expandability of the clay, which determines how tight the contact between clay and rock and clay and supercontainers and canisters will be.

Table 2: Typical geotechnical properties of natural soft smectitic clay barrier materials saturated with distilled water. The same clays saturated with Ca-rich water have about 100 times higher conductivity and 10 times lower swelling pressure (Pusch et al, 2019).

Clay	Dry density, kg/m ³	Hydraulic conductivity, m/s	Effective swelling pressure, MPa
Montmorillonite-rich (MX-80)	1,350	5E-12	1,020
Saponite-rich clay	1,230	4E-12	1,250
Muscovite/illite/montmorillonite mixed-layer clay	1,530	E-12	1,200

The table illustrates the importance of the density and type of smectite clay, illustrating also that the three candidate clays have approximately the same expandability and hydraulic conductivity but for quite different densities. Creep strain rate is also a function of the density and clay mineral composition and can be determined by unconfined compression tests under axial load. Following Pusch and Feltham (1980, 2015), the strain rate is appertaining to logarithmic creep for thermodynamically defined limits of the spectrum of energy barriers in the course of transient creep, implying creep strain to be proportional to $\log(t+t_0)$, where t denotes time after onset of creep and t_0 is a constant. The significance of this constant is that it indicates whether the microstructure is homogeneous and non-cemented or if interparticle clay bonds consist of chemical precipitations. If the latter conditions prevail and the precipitates are quartz or cristobalite these particles promote a high thermal conductivity (Figure 9).

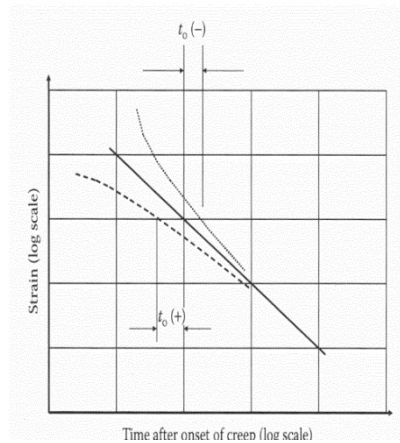


Figure 9: Generalization of creep curves of log-time type (After Pusch et al, 2019). $t_0=0$ means perfect logarithmic behaviour. Negative t_0 indicates brittle interparticle bonds by chemical precipitation.

4.3.3.3 Experimental

The clay materials investigated are proposed here as buffer clay candidates. They are commercially available bentonite clays from the US (MX-80), bentonitic saponite/palygorskite from Greece, and German mixed-layer (ml) Friedland Clay. Major data are given by the description below.

- MX-80 clay (dioctahedral), stemming from the montmorillonite-rich (70-90%) Cretaceous bentonites in Wyoming and South Dakota in USA, contains two general types of montmorillonite: i) those with normal charge as end member of IS-ml series, and ii) low-charge montmorillonite as end member of diVS-ml series. The ratio IS:diVS varies from 1/20 to 2/3, (Svemar, 2005 a and b; Kasbohm et al, 2012),
- Saponite/palygorskite (trioctahedral), sampled from Tertiary Greek bentonites, and investigated by XRD and TEM-EDX that indicate that both phases have low electric charge, strong expandability and high swelling pressure, thereby qualifying as buffer candidate for use in HLW repositories (Gueven, 1990; Pusch, 2008). This conclusion is in agreement with earlier findings from deep oil and gas drilling projects and national buffer clay studies. The investigated clay had been converted to Na form in the mineral processing plants.
- Mixed-layer muscovite/montmorillonite from north-eastern Germany is known by geologists as Friedland Ton (Clay) with a complex crystal structure consisting of sheets of muscovite or illite (30-60%) coupled to montmorillonite sheets (40-70%) via interlamellar space that is occupied by exchangeable cations and water molecules responsible for the particles' expandability (Herbert et al, 2008). The CEC is about 50meq/100g, which is about half of the capacity of pure montmorillonite. Such clays often have an appreciable content of chlorite that can serve a lubricator at compaction as exemplified by the Friedland Clay, which is known to be easily compactable, largely irrespective of the water content.

4.3.3.4 Buffer evolution under isothermal conditions

While hydration of the initially only partly water-saturated buffer clay involves only wetting, maturation includes microstructural evolution caused by physico/chemical particle interaction, relative motion of clay particles to reach a stable state under the prevailing environmental conditions with respect to groundwater composition and pressure, and temperature. For long-term modelling one needs to take chemical and mineralogical processes and impact of changes in effective pressure and creep into consideration, while for early stages of clay buffer evolution, the wetting of initially only partly water saturated material – including thermally generated chemical processes - and related changes in dry density are to be focused on.

Confining ourselves here to examine how swelling of buffer clay evolves upon water entry and uptake we conclude from comprehensive experiments that these processes generate compressive forces throughout the wetted portion, which will be transmitted to unwetted portions of the buffer clay, resulting in progressive compression of the latter parts (Pusch et al, 2019). For the continued maturation any difference in dry density anywhere within the clay causes migration of porewater

because the hydration potential, which depends on the transient degree of water saturation, is a unique function of the dry density. The impact of a significant thermal gradient is that ordered interlamellar hydrates break down causing increased mobility of the porewater and reduction of the swelling pressure (Pusch, 1993).

Several coupled processes take place in the maturation of the buffer clay that initially consists of partly water saturated dense aggregates of compacted clay granules. In strongly simplified form they can be described as follows:

- Water enters the deposition holes from the cold rock/buffer contact where the clay expands and exerts a swelling pressure on the drier clay that surrounds the hot canisters. The densified clay here sets up an increased hydration potential, which initiates migration of water from the outer cold clay to the inner, heated clay. Here, hydration causes a swelling pressure that consolidates the colder part that was initially expanded,
- Transport of water in liquid form takes place from the cold towards the hot part of the buffer clay and causes partial vapourization followed by flow back in vapour form towards the colder part where condensation takes place followed by migration of water towards the warm side where vapourization takes place etc,
- Water redistribution is associated with changes in dry density and hydration potential meaning that the whole saturation period makes microstructural reorganization comprehensive and transient.

The integral effect of the various processes relates to the microstructural constitution inherited from the initial state of clay granules being compressed to form blocks. The smectite granules have a water content that depends on the relative humidity of the air in which they are being stored. It is usually about 10% for pure smectite stored at 50-70% RH, implying that the interlamellar space holds 1-2 hydration layers. The microstructural evolution of the system of granules, welded together by the very high compaction pressure, is controlled by water sucked up from the surroundings, firstly by capillary action of the widest microstructural channels and then by diffusive migration via smaller channels, and finally from parts with larger interlamellar space to tighter ones. The role of temperature is that heated interlamellar water will be less ordered and viscous and becomes expelled from this space in conjunction with contraction of the stacks of lamellae and growth of voids and channels (Pusch, 2015).

In this context we also need to touch on the issue of bringing the 5-10ton supercontainers down to the predetermined level in the 3km deep holes. This operation requires that the bearing capacity and wall friction resistance of the clay mud that fills the holes at the beginning of and during the individual placements, are exceeded. The initially only partly water saturated dense smectite blocks in the supercanisters undergo hydration and expansion by absorbing water from the mud as indicated in Figure 10 (Pusch et al, 2019, Yang et al, 2015). This means that the mud around the submerged supercontainers stiffens by losing water to the dense clay blocks, which successively become softer until the entire clay fill is ultimately

uniform or nearly so. The increased density of the mud being consolidated causes a rise in thermal conductivity.

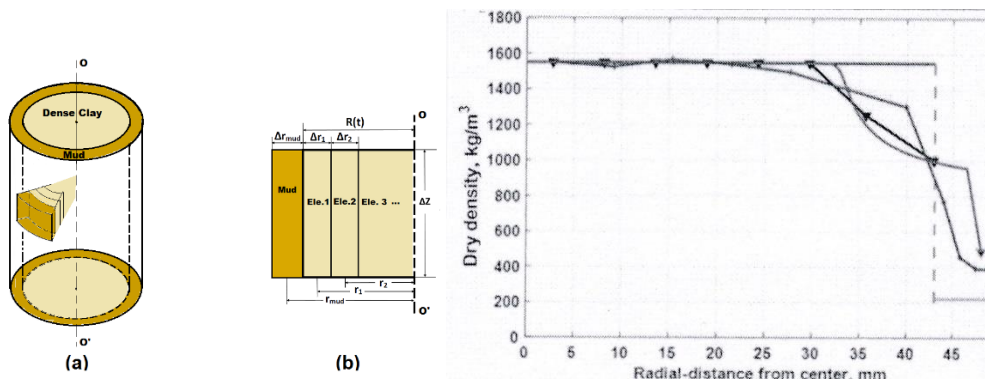


Figure 10: VDH physical model test for 12 hours without canister. a) shows dense, fully water saturated smectite clay core with 43mm radius surrounded by soft smectite mud with 7mm radial thickness. b) Redistribution of dry density indicating that the dense clay became softer within about 30mm distance from the symmetry axis while the mud extending from 43-50mm got its dry density increased from 200 to 400-1,000kg/m³ (Yang et al, 2015). Experimental data are dots, predicted values are triangles.

4.3.4 Physical and mineralogical evolution of buffer clay under hydrothermal conditions

Clay samples, representing the three reference buffer clay materials, were kept in hydrothermal copper cells (oedometers) for 8 weeks with 95°C temperature at one end, and 35°C at the opposite, for identifying changes in mineralogy and geotechnical properties. The treatment involved circulation of 1.0% CaCl₂ solution through a filter at the cold end (cf. Figure 11). At the end of the tests, the samples were sliced into three parts, which were tested with respect to chemical and mineral composition, and to their geotechnical performance, i.e. hydraulic conductivity and expandability.

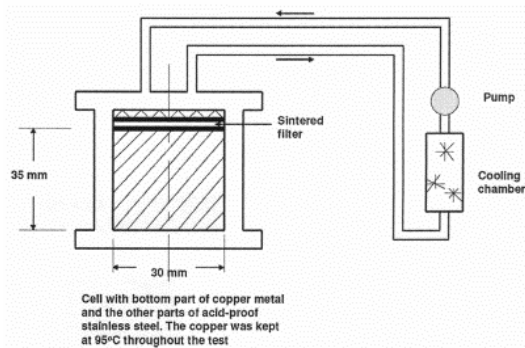


Figure 11: Test setup with cold end kept at 35°C and hot end at 95°C (Pusch and Yong, 2006; Kasbohm et al, 2012).

The 8-week laboratory study was a small-scale simulation of the conditions in the near-field of an HLW repository where the buffer clay is exposed to the heat from an enclosed HLW canister while being wetted by uptake of water from the surrounding colder rock. The initial dry density of the buffer clay was lower than under real conditions for speeding up physical and chemical processes and making possible changes obvious in reasonable time. The initial chemical and mineralogical compositions of the test samples are given in Table 2. Migration of dissolved copper into the three clays in the hydrothermal experiments of compacted clay was investigated as well (Kasbohm et al, 2012).

At the end of the tests the samples were sliced into three parts which were tested with respect to dry density, hydraulic conductivity, expandability (swelling pressure), and chemical composition. As indicated in Table 1 the dry density increased next to the hot boundary and dropped in the coldest part. The increase in density is ascribed to compression in the early hydration phase when the swelling pressure quickly rose in the cold parts of the sample, which became water saturated first. For MX-80 clay the swelling pressure had dropped very strongly in the hottest part while it was roughly the same as of untreated MX-80 clay in the central and cold parts for the respective densities. This indicates that the swelling pressure of the most heated part, which should have been sufficient to compress the softer, colder parts of the sample, had in fact become significantly reduced. The hydraulic conductivity of this part was about 100 times higher than that of untreated MX-80 clay but only slightly higher than of the mineralogically and chemically almost unaffected clay in the central and cold parts. The change in hydraulic conductivity can be explained by microstructural collapse, preserved by cementation of Si precipitates. Thus, the microstructure of the hot part appears to have larger particle aggregates and larger voids than the central and cold parts (Figure 12).

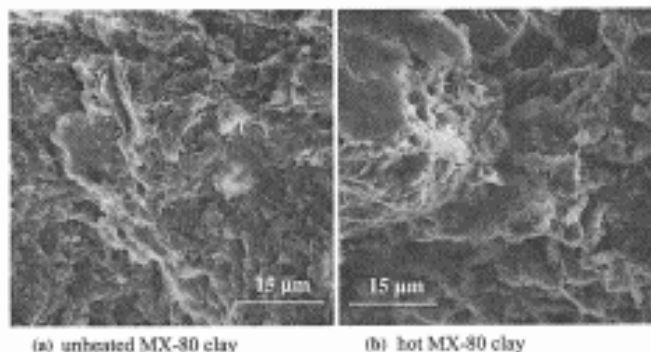


Figure 12: Scanning electron micrographs (SEM) of unheated (left) and hydrothermally treated MX-80 clay with larger particle aggregates and voids and silicious precipitation (right).

XRD analysis showed that the montmorillonite content of MX-80 was mainly unchanged by the hydrothermal treatment and that the only obvious process was some very slight formation of illite in the hot region. TEM-EDX analyses indicated, however, that most of the montmorillonite particles had undergone alteration, i.e. from montmorillonite into two different series of mixed-layer phases: IS-ml and diVS-ml phases (Kasbohm et al, 2012). For the latter it had the form of enrichment of Al in the octahedral sheet and of illitization. For the mixed-layer clay this process, implying reduction of the montmorillonite content, is indicated by the different ratios of montmorillonite layers in the mixed-layer series.

The outcome of the tests showed that while saponite was nearly unchanged and had not taken up any copper, while MX-80 had undergone substantial changes in physical performance and had adsorbed significant amounts of copper. The mixed-layer Friedland clay was intermediate in both respects (Table 3). Saponite was hardly changed at all and did not react with metallic copper. The data for the 18-32mm distance from the hot boundary, i.e. the coldest part of the samples, represent the natural materials.

Table 3: Properties of MX-80, saponite-rich DA0464 and Friedland clays at different distance from the hot boundary after 8 weeks hydrothermal tests at 95 °C in contact with Cu-metal.

Clay	Distance from hot boundary, [mm]	Temperature [°C]	Initial dry density/Final density [kg/m ³]	Initial /Final hydraulic conductivity [m/s]	Initial /Final swell pressure [MPa]	Chemical composition of natural material in weight percent SiO ₂ /Al ₂ O ₃ /Fe ₂ O ₃
MX-80	0-7	85-95	1.353/1.380	2E-11/2E-13	4.00/0.15	55/25/3
	7-18	50-60	1.353/1.350	5E-12/3E-11	1.02/1.00	-
	18-32	35-45	1.353/1.270	8E-12/E-11	0.60/0.45	-
Saponite	0-10	85-95	1.237/1.380	E-12/E-11	2.00/1.88	55/12/11
	10-19	50-60	1.237/1.170	5E-12/E-11	1.30/1.28	-
	19-32	35-45	1.237/1.175	4E-12/8E-11	1.30/1.17	-
Friedland	0-8	85-95	1.527/1.725	E12/5E-11	1.00/0.24	53/18/5
	8-21	50-60	1.527/1.545	2E-11/2E-11	0.63/0.45	-
	21-32	35-45	1.527/1.360	5E-11/5E-11	0.45/0.30	-

The fact that the properties of the saponite-rich clay were unaltered is in good agreement with the observations from Lan's experiments with Fe-clay (Herbert et al., 2016). Deep corrosion (>1mm) of the copper cells and migration into the MX-80 clay by more than 1 mm depth were linked to the remarkable change of its physical performance in comparison with the mixed-layer clay, which is an Fe³⁺-rich illite/montmorillonite clay with about 70% montmorillonite. Strong corrosion of copper contacting the MX-80 clay was noticed (Pusch and Yong, 2006; Kasbohm, 2012).

The overall conclusion was that the investigated saponite clay suffered less from the hydrothermal treatment than the montmorillonite-rich MX-80 clay and that the mixed-layer clay was intermediate in this respect. The MX-80 clay sorbed substantial amounts of copper to a significant distance from the copper plate. Saponite and the mixed-layer clay did not take up any copper at all or very little. The distribution of Cu in MX-80 and mixed-layer clay mirrored advective transport in channels formed by coupled voids. This can be explained by applying the synthesized model by Herbert et al. (2012), and Herbert (2016), according to which MX-80 should be smectite destabilized by 50 %, while the mixed-layer clay should be smectite destabilized by 15% (low effect caused by Si-precipitation yielding cementation), and the saponite-rich clay be totally unaltered.

On adapting Lan's Fe-corrosion model (cf. Kasbohm, J., Pusch, R., Thao Hoang-Minh, 2012), to copper, one would find that copper and copper oxide should be adsorbed on the edges of smectite particles, which are positively charged for

moderate and neutral pH-ranges. This causes reduction of structural Fe^{3+} in smectite clay and migration of Fe and Cu ions into smectite interlayers to compensate for the increased layer charge deficit.

In this context it is appropriate to indicate what the interaction would be of smectite clay and metallic iron and steel, which are canister candidate materials in several countries that have to dispose their HLW. This matter has been thoroughly investigated in comprehensive studies of which a joint French/Swedish project will be used here as reference. It was planned and executed in a similar manner as the described study of the three smectite clays confined in copper cells but also included a test with gamma radiation acting on them. Cylindrical 7cm long MX-80 samples with a dry density of $1,650\text{kg/m}^3$ were confined in cells with an iron plate at the heated end and a water saturated filter at the opposite one (Pusch et al, 1993). Weakly brackish water with Na as dominant cation and very little potassium (<10 ppm) was circulated through the filter that was kept at 90°C . The iron plate was heated to 130°C and kept pressed under 1.5MPa during the 1-year experiments. In one of the tests a gamma radiation dose of about $3\text{E}7\text{Gy}$ acted on the iron plate, the adsorbed radiation dose being $3,972\text{Gy/h}$ at the hot plate contact, to around 700Gy/h at half length of the sample, and to 456Gy/h at the coldest end. The investigation of the samples comprised XRD analysis, electron microscopy with EDX, chemical analysis, infrared spectrometry IR, and CEC determination.

The analyses showed that the main mineralogical changes taking place in the hot part of the samples were disappearance of feldspars, amphibole, and some of the quartz and smectite. However, there was nearly no difference between the sample exposed to radiation and the one that was not irradiated, except that Fe migrated from the iron plate into the clay somewhat quicker under radiation. In comparison with untreated MX-80 clay, hydrothermal treatment with and without radiation gave insignificant chemical changes, which was also supported by CEC data. They showed that untreated MX-80 had $\text{CEC}=99\text{meq}/100\text{g}$ while the most strongly heated and radiated clay had $\text{CEC}=93\text{meq}/100\text{g}$. However, creep testing at room temperature of samples from various distances from the hottest end gave witness of significant stiffening (Figure 13). Thus, the shear strain of the sample exposed to 130°C was about 3 times smaller than for the one heated to 90°C . Table 3 shows that some minor loss of montmorillonite took place at $115\text{-}130^\circ\text{C}$ while the loss of feldspars was considerable. Gypsum, kaolinite, quartz and chlorite were formed in the most heated part, indicating that such precipitations, together with coagulation of the smectite particles, caused the strengthening and stiffness.

In summing up one finds that the changes in mineral composition were similar for the MX-80 analyses using copper and iron cells, and that the general formula for degradation of smectites is valid for temperatures exceeding 60° to 70°C :

$$S + (Fk + Mi) = I + Q + Chl \quad (1)$$

where S denotes smectite, Fk potassium feldspars, Mi micas, Q quartz and Chl chlorite. Pytte/Reynold's and Grindrod/Takase's rate equations for conversion of smectite to illite are hence deemed applicable:

$$dS/dt = [Ae^{-U/RT(t)}] [(K+/Na+)mSn] \quad (2)$$

where U=activation energy, S=mole fraction of smectite in I/S assemblages (S=smectite, I=illite), R=universal gas constant, T= absolute temperature, t=time, m,n= coefficients.

Assuming the loss in isolation potential of the buffer material to be inversely proportional to the smectite content, we find this loss to be as specified in Table 4 for MX-80-type clays exposed to an average temperature of less than 130-150°C. The probable mechanisms involved in chemical and mineralogical changes of smectites is indicated in Figure 14.

Table 4: Mineralogical changes in one year long hydrothermal tests of MX-80.

M=Montmorillonite, F=Feldspars, G=Gypsum, Q=Quartz, K=Kaolinite, Chl=Chlorite, I=Illite. +++ means strong increase, ++ significant increase, + slight increase, --- strong loss, -- significant loss, - slight loss. 0 means no change.

Treatment	125-130°C	115-120°C	105-110°C	90-95°C
Hydrothermal without radiation	M -	M -	M 0	M 0
	F ---	F --	F -	F -
	Chl+	Chl +	Chl 0	Chl 0
	G ++	G +++	G +	G+
	K ++	K +	K 0	K -
	Q +	Q +	Q 0	Q 0
	I +	I 0	I 0	I 0

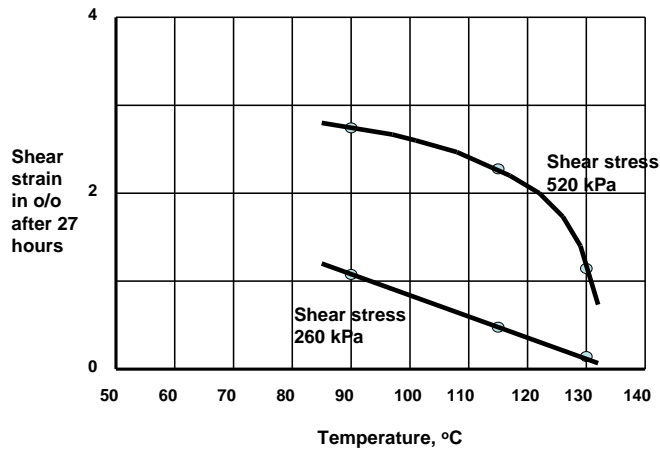


Figure 13: Shear box testing of MX-80 clay from hydrothermal experiment without radiation. Normal pressure 6 MPa. The accumulated strain of the 90°C part was 2.7% for the shear stress 520kPa and 1.0% for the shear stress 260 kPa. Hydrothermal treatment by 130°C gave 1.1 % strain for 520kPa and 0.2 % strain for 260kPa.

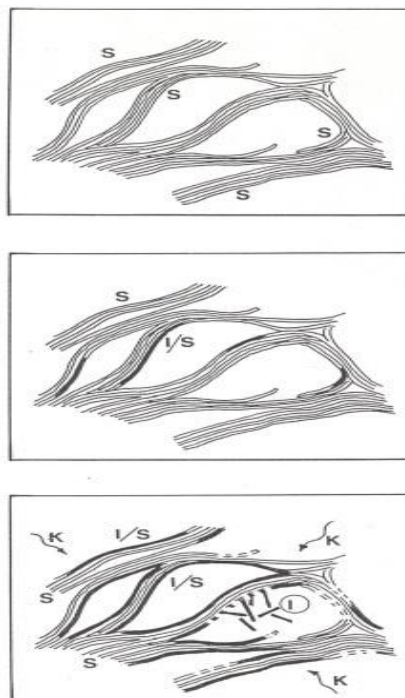


Figure 14: Smectite-to-illite conversion via mixed-layer I/S formation and/or direct precipitation of illite. The dark contours represent precipitations of silica and/or illite (Pusch, 1994).

4.3.5 Concrete in deep holes

Concrete will be used for stabilization of deep deposition holes as indicated in Figure 15. Ordinary concrete with Portland cement as binder would be short-lived and degrade contacting clay seals, while use of low-pH cement and inorganic superplastizicers (talc) that do not give off colloids that can transport radionuclides, will do. The cement/clay reaction products contribute to the strength of the concrete and the relatively low pH, i.e. about 10 of the concrete porewater (cf. Muhammed et al, 2014), minimizes the degrading effect of concrete that directly contacts clay seals.

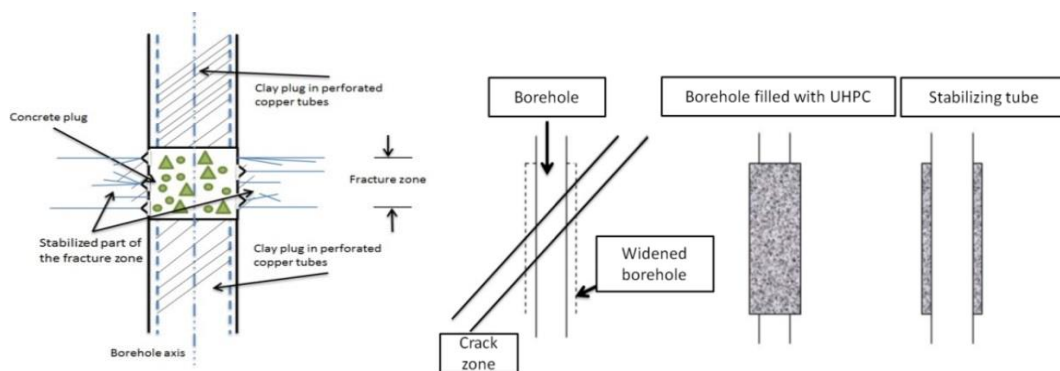


Figure 15: Use of concrete in VDH. Left: Concrete plugs in boreholes for stabilization and hindering of clay particles from migrating into the fracture (crack) zone. Right: construction of concrete plug under water (“UHPC”) by casting in reamed hole and final re-boring and filling with concrete or supercontainer submerged in smectitic clay mud.

An early recipe proposed in SKB’s Borehole Sealing Program (Pusch et al, 2007) had the following components in kg per cubic meter of concrete: Portland cement (60kg), silica fume (60 kg), fine-quartz (200kg), fine cristobalite (200kg), Glenium 51 superplasticizer (4.4kg in dry form), granitic aggregate 0-4 mm (1,700kg), and water (244.3kg). The compressive strength was 4.5MPa after 2 days and 31.7MPa after 28 days at room temperature. Such concrete, having pH>12, was cast on top of a clay seal in a 76mm borehole, and analyzed after about 3 years with respect to the mineralogy and chemical composition of both clay and concrete. This showed significant degradation of both, by dissolution and cation exchange from Na to Ca of the clay, and by dehydration and fissuring of the concrete (Warr and Grathoff, 2010). These observations and the probability that organic fluidizers will degrade or be eaten by microbes led to the following composition for the laboratory study: low-pH cement⁶, quartz aggregate, and talc as fluidizer. The respective contents were: cement 6.5%, talc 9.5%, and aggregate 84% (100% <4 mm, 93% <2mm

⁶ MERIT 5000 which has 34% SiO₂, 13% Al₂O₃, 17% MgO and 31% CaO.

70 % < 1mm, and 30% < 0.1 mm), (Pusch, et al., 2013). A suitable water/cement ratio can be 3-4 for this composition having an aggregate/cement ratio of 10-15. This gives 2,070 kg/m³ density and pH=10. Typical compressive strength data after 2-28 days of curing are summarized in Table 5, together with data for a corresponding concrete with Portland cement.

The microstructural constitution of this type of concrete reflects the plastic behaviour of the talc phase in the earliest curing phase: the formation of skin coatings of quartz grains by flaky talc particles results in easy glide of both. The subsequent strengthening provided by the talc is caused by precipitation of cementing complexes formed by reactions between low-pH cement components and slowly dissolving talc. The hydraulic conductivity was measured after 7 and 21 days giving K-values of 5E-9 and 8E-10 m/s, respectively (Mohammed et al, 2014). The described grain-size distribution of the aggregate and the very low cement content gives a tight microstructure that is similar to bottom moraine and minimizes changes in physical performance of the concrete in the unlikely case of complete loss of the cement (Mohammed et al, 2013). Thus, the concrete has a very low compressibility and a pore size distribution that minimizes the risk of infiltration and through-transport of clay particles from contacting clay seals. The longevity of the magnesium/silicate cement reaction products from talc/cement interaction is believed to make total loss of the cement improbable.

The major difference between cement with and without talc is a loss in F, Al, S, and K and an increase in Na and Mg in the presence of talc. Compared with talc-free cement a significant increase in Ca, Mg and Si and decrease in Al were the most obvious findings. They indicate that the talc component was partly dissolved, and the elements incorporated into new cementing compounds created in the first week of reaction. Further reactions caused the obvious strengthening recorded after 28 days. The results also indicate that the dissolution of talc provided additional Mg for the cementing precipitates. It is estimated that complete curing, involving dissolution, diffusive migration of mobile elements and successive precipitation of reactive elements in the chemically transient porewater, can take years and decades and even longer time in big seals in large-diameter holes. The binding components of the talc concrete provide high strength with time and the use of crushed quartzite as aggregate implies longevity.

Table 5: Average uniaxial compressive strength in MPa of low-pH concrete prepared with 6 % cement content (Mohammed et al, 2014).

Curing, (days)	Portland, cement	Merit 5000 (low-pH cement)
2	0.5-0.6	0.01-0.02
7	0.6-0.7	0.1-0.4
28	0.8-0.9	1.8-2.7

4.3.6 Gas formation

Specific studies have indicated that gases can be generated from the direct contact of possible repository brine and radioactive waste and cause significant build-up of pressure. Four factors have been identified which influence the production of gases: radiolysis, microbial activity, corrosion, and evolved residual.

The first mechanism, radiolysis of the water and material inherent in the waste and the brine, will result in the production of hydrogen (H₂), oxygen (O₂), nitrogen (N₂), carbon dioxide (CO₂), carbon monoxide (CO), nitrous oxide (N₂O), and small organic compounds. The corrosion mechanism will result from the electrochemical potential differences of canister/container metals in water and brine. The bacterial degradation of organic and inorganic material in the waste is an additional mechanism that could also result in the production of methane (CH₄). The final mechanism is the generation of air (N₂, O₂, and CO₂) in the waste that will evolve to some equilibrium concentration within the repository (Kasbohm et al, 2012).

5. Comments and conclusions

5.1 General

The described concept implying combination of deep boreholes with heat-producing highly radioactive waste, and equally deep boreholes for utilizing the waste-generated heat, has the advantage of taking care of the waste in a manner similar to other methods for deep disposal of such waste but with a potential to create geothermal energy or electric energy. One waste-bearing hole can have 200 canisters producing 600 to 1,800W or around 1,200 to 3,600kW per hole and assuming that at least one tenth of this can be picked up by the 3km deep hot water-holes bored between the holes with waste, they would deliver an energy of about 0.3 to 0.9 million kWh per year. Since a VDH repository is estimated to host 10 to 20 waste-bearing holes and the same number of hot water holes it would produce an annual amount of energy of no less than 10 million kWh per year, which would suffice to warm several large industrial buildings for only the cost for the maintenance and repair required by running heat exchangers and pumps. This estimate suggests that the proposed system is profitable.

The safety criteria that have to be fulfilled imply that no release of radionuclides must take place until after 10,000 to 100,000 years after waste placement depending on and specified by national legislation. An often claimed difficulty is how measurement of possible radioactive leakage can be detected and done with. Own experience and IAEA's aspects suggest, however, that one shall refrain from installing instrumentation because of the risk that cables can serve as pathways for water and possibly released radionuclides.

5.2 Disposal of the radioactive waste in the form of spent reactor fuel

The basic idea of deep geologic disposal of radioactive waste of the described VDH type is to store it at a depth where the density, heaviness and fluidity of the groundwater are high enough to inhibit possibly contaminated groundwater in the deployment zone to move up to the biosphere. At the intended depth, the hydraulic conductivity of crystalline rock is very low and the regional hydraulic gradients insignificant as well, except in major fracture zones in which no waste disposal should be made. Minor fracture zones cannot be avoided in locating the deep boreholes for waste disposal and utilization of waste-heated water. Where the holes pass through such zones the rock material is excavated under water and replaced by erosion-resisting and chemically stable low-pH concrete. All construction work takes place under water and waste handling is made remotely in soft smectitic clay mud in which the supercontainers are submerged in the last phase of the waste placement.

The sealing components in the waste-bearing holes consist of precompacted dense smectite-rich (“buffer”) clay confined, together with canisters with spent nuclear fuel, in perforated supercontainers of copper, Navy Bronze or titanium⁷. According to the comprehensive research work made in Sweden and various other countries using nuclear energy, the mechanical and chemical/mineralogical stability of smectitic buffer clay under the hydrothermal conditions prevailing to about 3km depth is sufficiently good for guaranteeing safe function for many tens of thousands of years. The concept implies that the holes above the deployment zone, i.e. over 1,500m depth, will be located in rock with significantly lower temperature (70-80°C) than in the deployment zone (up to 150°C), meaning that the clay-sealed upper parts of the holes will be exposed to less demanding conditions and have a waste-isolating ability that is typical of many bentonite clays found in nature.

5.3 Utilization of waste-heated groundwater

The possibility to utilize the waste-generated heat energy of groundwater circulated in separate systems of deep boreholes depends on the amount of natural heat energy that is provided by the groundwater mass in the host rock added by the energy transferred from the waste-bearing holes. The natural groundwater has a temperature of 30-50°C from 1,500 to 2,000m depth which will not be much changed by placing the waste in the holes in this depth interval.

Safety issues

An issue of importance is that international rules concerning control and book-keeping of fissile material, nuclear safeguards, and use of an adequate system for such control, should be operational until the fissile material is practically irrecoverable. This would require, according to IAEA, monitoring of repositories for spent fuel against unauthorized extraction or movement of the disposed material after closure of repositories of mined type because of relatively easy access via

⁷ Special steel or alloys may serve but require long-term testing and qualified chemical/mineralogical modelling

ramps and shafts. For VDH, monitoring would not be possible because of the deep location of the waste and would not be required because of the small waste “charge” per hole.

6. Acknowledgement

Professor emeritus Sven Knutsson at Luleå University of Technology is greatly indebted for valuable discussions on thermal properties of rock and clay.

References

- [1] Brady, P.V., Arnold, B.W., Freeze, G.A., Swift, P.N. Bauer, S.J., Kanney, J.L., Rechar, R.P., Stein, J.S (2009). Deep borehole disposal of high-level radioactive waste, SANDIA REPORT 2009-4401, New Mexico/Livermore Calif. USA, 2009.
- [2] Grindrod, P. and Takase, H. (1993). Reactive chemical transport within engineered barriers. In: Proc. 4th Int. Conf. on the Chemistry and Migration Behaviour of Actinides and Fission Products in the Geosphere, Charleston, SC USA, 12-17 Dec. Oldenburg Verlag 1994 (pp. 773-779).
- [3] Grundfelt, B. (2010). Jämförelse mellan KBS-3-metoden och deponering i djupa borrhål för slutligt omhändertagande av använt kärnbränsle (Comparison of the KBS-3 Method and deposition in deep boreholes), Swedish Nuclear Fuel and Waste Management Co (SKB), Stockholm, R-10-13, 2010.
- [4] Gueven, N., Huang, W-L. (1990). Effects of Mg^{2+} and Fe^{3+} substitutions on the crystallization of discrete illite and illite/smectite mixed layers. Dept. Geosciences Texas Tech University, Exxon Production research Co, Houston, Texas, USA.
- [5] Herbert, H.-J., Kasbohm, J., Nguyen-Thanh, L., Meyer, L., Hoang-Minh, T., Mingliang, X., Ferreiro/ Mählmann, R. (2016). Alteration of expandable clays by reaction with iron while being percolated by high brine solutions. *Applied Clay Science* 121–122 (2016) 174–187.
- [6] Kasbohm, J., Pusch, R., Lan Nguyen-Thanh, Thao Hoang-Minh (2012). Lab-scale performance of selected expandable clays under HLW repository conditions. *Environmental Earth Sciences*, Vol 69, No 8.
- [7] Mohammed, M. H., Pusch, R., Al-Ansari, N., Knutsson S., Emborg, M., Nilsson, M., and Pourbakhtiar, A. (2014). Talc-Based Concrete for Sealing Borehole Optimized by Using Particle Packing Theory. *J. of Civil Engineering and Architecture*, Apr. 2013, Volume 7, No. 4, pp. 440-455.
- [8] Pusch, R. and Börgesson, L. (1992). Performance assessment of bentonite clay barrier in three repository concepts: VDH. KBS-3 and VLH. Pass Project on Alternative Systems Study, SKB Technical Report TR 92-40, Swedish Nuclear Fuel and Waste Management Co (SKB), Stockholm.

- [9] Pusch, R. (1993). Evolution of models for conversion of smectite to non-expandable minerals. Technical Report TR93-33, Swedish Nuclear Fuel and Waste Management Co (SKB), Stockholm.
- [10] Pusch, R. (1994). Waste disposal in rock, *Developments in geotechnical engineering*, 76. Elsevier Publ. Co., ISBN: 0-444-89449-7.
- [11] Pusch, R., Feltham, P.A. (1980). A stochastic model of the creep of soils, *Geotechnique*, 30, 497-506.
- [12] Pusch, R. and Yong, R.N. (2006). *Microstructure of smectite clays and engineering performance*. Taylor & Francis, New York, London.
- [13] Pusch, R., Kasbohm, J., Pacovsky, J. and Cechova, Z. (2007). Are all smectite clays suitable as ‘‘buffers’’? *Phys Chem Earth Parts A/B/C*.
- [14] Pusch, R. (2008). *Geological storage of radioactive waste*, Springer-Verlag, Berlin, Heidelberg, (ISBN: 978-3540-77332-0).
- [15] Pusch, R., Yong, R.N., Nakano, M. (2019). *Geologic Disposal of High-Level Radioactive Waste*. CRC Press, Taylor and Francis Group, London, New York.
- [16] Pusch, R., Warr, L., Grathoff, G., Pourbakhtiar, A., Knutsson, S., Mohammed M. H. (2013). A talc-based cementpoor concrete for sealing boreholes in rock. *Engineering Geology*, Vol.5 (pp.251-267).
- [17] Pusch, R. (2015). *Bentonite Clay*, CRC Press (Taylor & Francis Group), ISBN 13:978-1-4822-4343-7.
- [18] Pytte, A.M. and Reynolds, R.C. (1989). The thermal transformation of smectite to illite. In: *Thermal History of Sedimentary Basins*. N.D. Naeser & T.H. McCulloh, eds. Springer Verlag (133-140).
- [19] Svemar, C. (2005a). Prototype repository project. Final Report of European Commission Contract FIKW-200000055, Brussels, Belgium
- [20] Svemar C. (2005b). Cluster repository project (CROP). Final Report of European Commission Contract FIR1CT-2000-20023, Brussels, Belgium.
- [21] Warr, L.N. and Grathoff, G.H. (2010). Sealing of investigation boreholes: Mineralogical and geochemical borehole plug analyses. Technical Report, Swedish Nuclear Fuel and Waste Management Co., Ernst-Moritz-Arndt Universität, Greifswald, Germany.
- [22] Yang, T., Pusch, R., Knutsson, S., Liu, X. (2015). Lab testing of method for clay isolation of spent reactor fuel in very deep boreholes. In: *Proc. World Multidisciplinary Earth Sciences Symposium - WMESS 2015*", September 7-11, Prague, Czech Republic.